*Computer Methods in Biomechanics and Biomedical Engineering*, Vol. 4, pp. 281–289
Reprints available directly from the publisher
Photocopying permitted by license only



# Multiaxial Mechanical Behavior of Human Saccular Aneurysms

P. SESHAIYER[a], F. P. K. HSU[b], A. D. SHAH[c], S. K. KYRIACOU[d] and J. D. HUMPHREY[a,*]

[a]*Biomedical Engineering Program, Texas A&M University;* [b]*Neurosurgery, Oregon Health Sciences University;* [c]*School of Medicine, University of Maryland at Baltimore;* [d]*Division of Neuroradiology, Johns Hopkins University*

*(Received in final form 20 May 2000)*

Intracranial saccular aneurysms are focal dilatations of the arterial wall that usually occur in or near the circle of Willis. Two-to-five percent of the population in the western world likely harbors such an aneurysm, rupture of which is the leading cause of non-traumatic subarachnoid hemorrhage. It is widely thought that these lesions rupture when wall stress exceeds wall strength. Given that aneurysms experience multiaxial stress and strain fields *in vivo*, there is a pressing need for data on their multiaxial mechanical properties. In this paper, we report the first multiaxial data on human saccular aneurysms. Lesions were obtained at autopsy, cannulated, and subjected to cyclic pressurization using a triplane video-based experimental system. The latter recorded the pressures and associated motions of multiple markers that were affixed to the surface of the lesion. Finally, a new sub-domain inverse finite element method was used to estimate the best-fit material parameters in a Fung-type pseudostrain energy function. It was found that the lesions were much stiffer than previously thought, which in turn will affect significantly any estimation of wall stress. There remains a need, however, to collect data on additional specimens, to evaluate different descriptors of the multiaxial behavior, and to correlate these findings with direct measures of the underlying histology.

*Keywords*: Stress–strain; Constitutive relation; Strength; Material properties

## INTRODUCTION

The mechanisms by which intracranial saccular aneurysms enlarge and rupture remain unknown, yet it has long been accepted that mechanics plays a key role [1–3]. For example, these lesions likely enlarge due to a growth and remodeling process that is controlled by hemodynamically-induced intramural and wall shear stresses; they likely bleed or rupture catastrophically in regions where the wall is weakened due to the upregulation of proteases, that is where multiaxial wall stress

* Address for correspondence: Biomedical Engineering Program, 233 Zachry Engineering Center, Texas A&M University, College Station, Texas 77843-3120. Tel.: 979-845-5558, Fax: 979-845-4450, e-mail: jdh@acs.tamu.edu

exceeds wall strength. Fundamental to understanding many aspects of the natural history of these lesions, therefore, are constitutive relations for the aneurysmal wall. There are five general steps in the formulation of any constitutive relation: delineation of the general characteristics of the material, establishment of an appropriate theoretical framework, identification of a specific functional form of the relation, calculation of best-fit values of the material parameters, and evaluation of the predictive capability of the relation.

Non-complicated, juvenile aneurysms are typically thin-walled, consisting primarily of multiple layers of types I and III collagen [4]. This collagen is distributed within the lesion such that the mechanical behavior is both anisotropic and heterogeneous [5, 6], and of course nonlinear over finite strains [7]. As a result, it appears reasonable to treat such aneurysms as nonlinear pseudoelastic membranes [8, 9]. Unfortunately, however, there has been no rigorous identification of a specific form of a constitutive relation for human aneurysms, primarily due to the scarcity of specimens and their non-axisymmetry.

In this paper, we present results from multiple regions on two non-axisymmetric human saccular aneurysms based on an assumed form of a pseudostrain-energy function – a Fung-type exponential. Best-fit values of the associated material parameters were determined herein from computer-controlled inflation tests by using a new sub-domain inverse finite element method to interpret the multiaxial data. Based on these results, it appears that saccular aneurysms are much less distensible at physiologic pressures than originally thought and they exhibit regional variations in their anisotropy.

## METHODS

### Experimental Device

Our specially designed system is described in detail elsewhere [10]. Briefly, it consists of two computers, a syringe pump, two pressure transducers, three CCD cameras and B&W monitors, a color frame-grabber board, an A/D board, and custom video analysis software (Fig. 1). Specimens

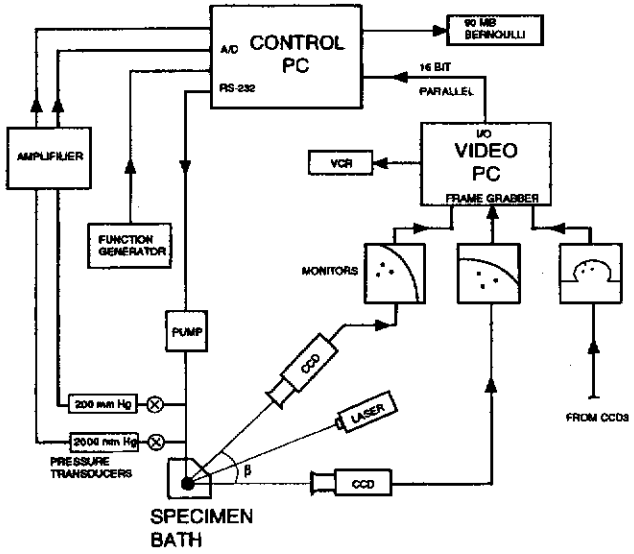


FIGURE 1 Schema of the experimental system. Note that the laser is used simply for alignment and calibration, not testing. Moreover, only the biplane cameras were used here due to the non-axisymmetry of the lesions studied (with permission).

are immersed in a physiologic saline solution, within a plexiglas chamber, and inflated by the computer-controlled syringe pump with the same solution. The "video PC" tracks the resulting motions of 3–6 closely spaced markers, which are affixed to the surface of the specimen, via two CCDs that are mounted coplanarly in biplane fashion. In cases of axisymmetry, the profile of the lesion can be determined via a third CCD (not shown), which is mounted orthogonal to the plane containing the other two cameras, and an edge-detection algorithm. Data (*i.e.*, the distension pressure and marker locations) are collected on-line at 15 Hz, which is sufficient given slow cyclic tests (at 0.01 Hz). Resolution was 0.25 mmHg and ~10 microns, respectively.

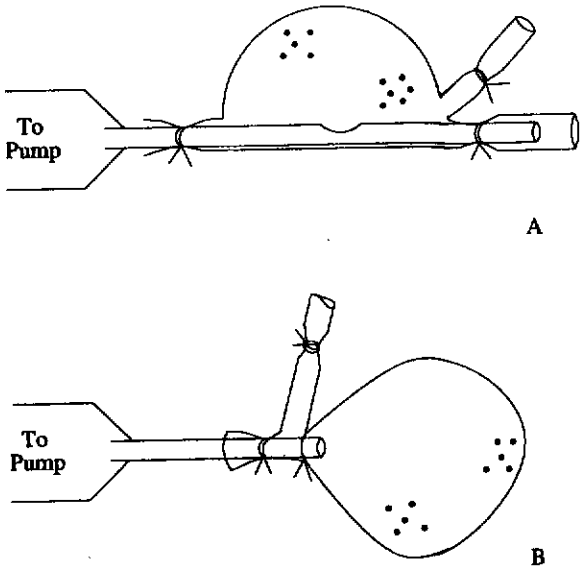


FIGURE 2 Schema of the mounting of a lesion within the system. The modified blunt ended needle was attached to a three-way stopcock, which in turn was supported by a plate and micro-manipulator. Note the multiple surface markers which define a region of interest.

### Specimen Preparation and Testing

Human intracranial saccular aneurysms were obtained at autopsy within 24 hours of death and transported to the laboratory in a cold normal saline solution. Once in the lab, they were placed in a $Ca^{++}$-free solution at room temperature (in mM): 116.5 NaCl, 22.5 $NaHCO_3$, 1.2 $NaH_2PO_4$, 2.4 $NaSO_4$, 4.5 KCl, 1.2 $MgSO_4$: 7 $H_2O$ and 5.6 dextrose. Perforating vessels in and near the lesion were ligated with 6-O to 9-O silk, depending on the size of the vessel, and the parent vessels were trimmed in length. The primary inflow vessel was cannulated with a blunt ended needle in one of two configurations depending on the geometry of the lesion (Fig. 2), and outflow vessels were ligated with 3-O or 4-O silk once any remaining blood was flushed out and the specimen was filled with the solution. Small black markers were placed on the surface via the splattering of waterproof ink; this avoided the necessity of applying glue to the lesion. The splattered ink resulted in redundant markers, but ample numbers from which to pick sets of 4–6 within multiple local regions of interest. The needle holding the lesion was then mounted within the test chamber on a three-way stopcock: one line communicated with the syringe pump and one with the pressure transducer. The stopcock, in turn, was mounted on a plexiglas plate that was held from above by a *x-y-z* micro-manipulator. The latter allowed the lesion to be moved within the field of view of the two biplane cameras so as to focus separately on different regions of interest. Once mounted and focused, marker locations were registered in the unloaded configuration (*i.e.*, just prior to collapse) and cyclic inflation tests begun.

Testing was accomplished in a conservative manner: first with cyclic inflations from ~3–50 mmHg, then 3–80 mmHg, and finally 3–130 or 3–150 mmHg. In each case, the specimen was preconditioned (5–7 cycles) prior to data collection. Once data were collected from one region, the specimen was reoriented via the micro-manipulator and/or rotation of the needle on the stopcock, and similar data were collected for additional regions. The specimens were perfusion fixed at 100 mmHg with a 10% buffered formalin at the conclusion of testing.

To plot the pressure–stretch behavior, the 3-D positions of each of the tracking markers were

determined at each pressure from the corresponding 2-D positions in each of the two views using the method of McCulloch *et al.* [11]. These coordinate locations were then smoothed as a function of pressure using the method in Shah *et al.* [12] and used to calculate the components of the 2-D deformation gradient **F** using the methods in Hsu *et al.* [8]. Principal values of the Green strain $\mathbf{E}=(\mathbf{F}^T\cdot\mathbf{F}-\mathbf{I})/2$ and thus stretch were then determined by solving the simple eigenvalue problem.

### A Candidate Constitutive Relation

Hsu *et al.* [8] showed that specific forms of the response functions (*i.e.*, derivatives of the pseudo-strain-energy with respect to the Green strains) may be inferred directly from data for an axisymmetrically inflated membrane. Unfortunately, however, our lesions were non-axisymmetric. Hence, we were forced to simply evaluate a candidate relation with regard to its ability to fit data. Perhaps the most commonly used constitutive relation for biological soft tissues is the Fung-exponential. Indeed, Kyriacou and Humphrey [9] showed that the following pseudo-strain-energy function describes the limited data of Scott *et al.* [7] on human lesions reasonably well:

$$w=c(e^{Q}-1),\quad Q=c_1E_1^2+c_2E_2^2+2c_3E_1E_2 \qquad (1)$$

where $w$ is defined per unit surface area, not volume, $c$ and $c_j$ $(j=1,2,3)$ are material parameters, and $E_i$ are the principal physical components of the 2-D Green strain (*e.g.*, $i=1,2$ denote the circumferential and meridional directions in an axisymmetric lesion). Although Humphrey [13] recently showed that this relation is restricted in the degree of anisotropy that it admits, it is nonetheless a reasonable candidate descriptor. Note, too, that the form of $Q(\mathbf{E})$ in Eq. (1) can be generalized to:

$$Q=\alpha J_1^2+\beta J_2+\gamma J_1J_4+\delta J_4^2 \qquad (2)$$

where $J_1=\mathrm{tr}\mathbf{E}$, $J_2=\det\mathbf{E}$, and $J_4=\mathbf{M}\cdot\mathbf{E}\cdot\mathbf{M}$, where **M** defines the preferred direction and $\alpha$, $\beta$, $\gamma$ and $\delta$ are material parameters (with $c_1=\alpha+\gamma+\delta$, $c_2=\alpha$, $2c_3=2\alpha+\beta+\gamma$). Regardless, the physical components of the Cauchy stress resultant tensor **T** are given by [14]

$$T_{\alpha\beta}=\frac{1}{J}F_{\alpha\Delta}F_{\beta\Xi}\frac{\partial w}{\partial E_{\Delta\Xi}},\quad \alpha,\beta,\Delta,\Xi=1,2 \qquad (3)$$

where $J$ is the determinant of the 2-D deformation gradient **F**. Because the membrane is modeled via a 2-D theory, there is no need to enforce the incompressibility constitutively, which simplifies the subsequent finite element computations; incompressibility can be enforced kinematically in post-processing, however, to determine stretches in the out-of-plane direction where $\lambda_3=h/H=1/(\lambda_1\lambda_2)$ and $h$ and $H$ are the deformed and undeformed thicknesses, respectively. Of course, the Cauchy stress $t_{\alpha\beta}=T_{\alpha\beta}/h$.

### Sub-domain Method

The lack of axisymmetry also complicates the estimation of best-fit values of the material parameters (note: one often determines such parameters by minimizing the sum of the squares of the errors between calculated and "measured" stresses or stress resultants). Whereas the principal stress resultants can be inferred directly from measurable data (*i.e.*, distension pressure and local curvatures) in the axisymmetric case [10], such is not the case in non-axisymmetric lesions. Hence, we employed a recently developed sub-domain inverse finite element method [15] to calculate the best-fit values of the material parameters. Briefly, this method employs the finite element method to solve a displacement boundary value problem defined over a sub-domain that is demarcated by a set of closely spaced markers on the surface (Fig. 2). The experimentally measured marker locations, at each pressure, serve two functions: in the case of 5 markers, the outer four serve as displacement boundary conditions in the finite

element solution whereas the inner *one* serves as an experimental measurement to which the finite element solution can be compared in a nonlinear least squares sense. Because each marker is located by three coordinate values $(x_1, x_2, x_3)$, each supplies multiple pieces of information for comparing the theoretically computed and experimentally measured position. Moreover, collecting marker positions at multiple equilibrium configurations (*i.e.*, pressures) provides the over-determined equations needed in least squares estimations. Although details are in the original paper, briefly the sub-domain method was accomplished by minimizing (using a Marquardt–Levenberg algorithm available in the MATLAB platform) the following objective function $e$,

$$e = \sum_{k=1}^{m} \{(\mathbf{Y}_c(\mathbf{b}) - \mathbf{Y}_e) \cdot (\mathbf{Y}_c(\mathbf{b}) - \mathbf{Y}_e)\}_k \quad (4)$$

where $\mathbf{Y}$ denotes a position vector that locates the inner marker(s) with respect to a laboratory coordinate system, with the subscripts $c$ and $e$ denoting calculated (by finite elements) and experimentally measured, respectively. Specifically, herein

$$\mathbf{Y}_c(\mathbf{b}) - \mathbf{Y}_e = (x_{1c}(\mathbf{b}) - x_{1e}, x_{2c}(\mathbf{b}) - x_{2e}, x_{3c}(\mathbf{b}) - x_{3e}) \quad (5)$$

where the vector $\mathbf{b}$ contains the unknown material parameters, and $m$ is the number of pressurized configurations. We culled the data to 50 such configurations that spanned the minimum and maximum pressures in a particular test. It can be shown for Eq. (1) that the four parameters must be positive [14]; the regression must be constrained so as to admit only physically realistic values of the parameters.

### Interpretation of Results

It is difficult to assess anisotropy and heterogeneity by simply comparing tabulated values of the best-fit values of the material parameters in a nonlinear constitutive relation. Moreover, Humphrey and Yin [16] showed that it is not possible to interpret anisotropy from plots of biaxial stress–strain data except in the case of equibiaxial stretching. Due to boundary conditions at the neck, the only region of an inflated saccular aneurysm that might experience equibiaxial stretches is the fundus, which is expected to exhibit isotropic or near isotropic behavior anyway. Hence, lesion anisotropy cannot be interpreted directly from stress–strain data or best-fit parameters even if one has multiaxial results in an inflation test.

Inasmuch as a valid constitutive relation must give reasonable results for all deformations within the intended range, Humphrey [13] suggested that it is prudent to evaluate the behavior based on predicted responses to select biaxial stretching: equibiaxial and strip biaxial tests. For example, for a homogeneous deformation of the form $\mathbf{F} = \text{diag}[\lambda_1, \lambda_2]$, the principal stress resultants are,

$$T_1 = \frac{\lambda_1}{\lambda_2}\frac{\partial w}{\partial E_1}, \quad T_2 = \frac{\lambda_2}{\lambda_1}\frac{\partial w}{\partial E_2} \quad (6)$$

with $w$ defined in Eq. (1) (note: this assumes that the directions of principal stress and strain nearly coincide, which has been borne out in most in-plane biaxial tests on collagenous membranes, as, for example in [14]). Hence, one can compute and compare results for various deformations. Whereas the equibiaxial test ($\lambda_1 = \lambda_2 = \lambda$) is most useful in this regard, we also considered uniaxial stress tests since there are two such reports in the literature. In the latter, one prescribes a stretch ($\lambda_1$ or $\lambda_2$) and then computes the value of the other stretch ($\lambda_2$ and $\lambda_1$) that results in a zero stress in the appropriate direction. For example, for $\lambda_1 > 1$ and $T_1 > 0$, with $T_2 = 0$, we have from Eqs. (1) and (4) that,

$$T_2 = 0 = 2\frac{\lambda_2}{\lambda_1} c e^{Q}(c_2 E_2 + c_3 E_1) \rightarrow \lambda_2 = \sqrt{\left(1 - \frac{c_3}{c_2} 2E_1\right)}. \quad (7)$$

Moreover, given a similar relation for $T_1$, which must be non-negative, it is easy to show that

$c_1 c_2 - c_3^2 > 0$, which provides a further restriction on the values that the best-fit parameters can assume. The same restriction holds for $\lambda_2 > 1$ and $T_2 > 0$ with $T_1 = 0$.

## RESULTS

Experiments were performed on two human saccular aneurysms. One was obtained from a 36 year old male. It had formed at the juncture of the internal carotid and the circle of Willis, and was approximately 2.6 mm in gross outer dimensions and 16 to 44 μm in thickness, both measured at 100 mmHg pressure. Moreover, the lesion was transparent over much of its surface and there was no indication of atherosclerosis or thrombosis. The second lesion was from a 76 year old male. It had formed at the first major bifurcation of the right middle cerebral artery and was approximately 9 mm in outer dimensions and 72 to 212 μm in thickness, again at 100 mmHg. This lesion was markedly heterogeneous, however, with one yellowish, stiff lateral region indicative of atherosclerosis and one thin, transparent bleb near the neck.

Figure 3 shows the pressure-stretch response for one region in the first lesion. In addition to the characteristic nonlinear response, note the modest (less than 10%) but very different extensions in the two principal directions. This is in contrast to the data of Scott *et al.*, who reported (averaged) equibiaxial extensions of 18% at pressures of 100 mmHg.

Because of the nonlinear behavior, the best-fit values of the material parameters for a particular region varied depending on the pressure-range during testing (note: this emphasizes that all specimen-to-specimen comparisons should be over comparable pressures, which herein we took to be 3–120 mmHg). Table I shows the best-fit values of the material parameters for 2 regions from the first lesion and 3 regions rom the second lesion. Note the similarity, but differences, in the values within a region (*i.e.*, anisotropy), from region-to-region (heterogeneity), and from specimen-to-specimen. Note, too, that the root mean sum of the squares of the error between the measured and estimated position was on the order of $10^{-3}$ mm or smaller except for one region in the second lesion. In all cases, $T_{11}$ is approximately circumferential and $T_{22}$ approximately meridional.

Figures 4 and 5 show representative predictions of the response of each lesion (one region) given the values of the parameters in Table I and assumed equibiaxial stretches from 1 to 1.1 (heretofore, the data of Scott *et al.*, would have suggested a stretch of 1.2 to be a reasonable upper limit for aneurysmal extensions). Note the nonlinear, anisotropic behavior. Results based on the other sets of parameters were similar. Overall, 3 of the 5 results suggested that the meridional direction was stiffer than the circumferential direction; with regard to location, 3 of the 4 regions that

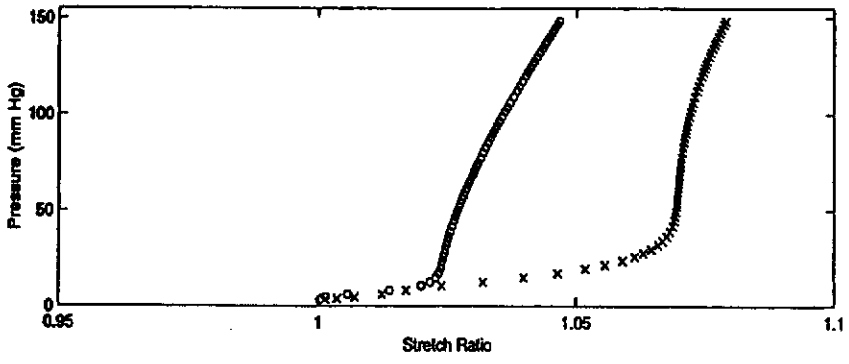


FIGURE 3 Pressure–principal stretch data for the loading cycle of one test on specimen $S_1$, one region.

TABLE I Best-fit values of the material parameters for different regions from each of the two lesions. $P_{max}$ (mmHg) denotes the maximum value of the pressure attained in the test, and RMS (mm) denotes the root mean squared error in the regression. Note that specimen 2 region 2 ($S_{22}$) was near an atherosclerotic region and thus significantly stiffer

| Lesion | $P_{max}$ | $c(N/m)$ | $c_1$ | $c_2$ | $c_3$ | RMS |
|---|---|---|---|---|---|---|
| $S_{11}$ | 80 | 7.02 | 3.28 | 15.65 | 3.04 | 6E−08 |
| | 120 | 9.13 | 3.61 | 17.13 | 3.31 | 6E−08 |
| $S_{12}$ | 80 | 12.60 | 10.74 | 13.08 | 11.02 | 2E−03 |
| | 120 | 16.70 | 12.16 | 14.81 | 12.47 | 4E−03 |
| | 150 | 19.51 | 13.00 | 15.85 | 13.34 | 7E−03 |
| $S_{21}$ | 80 | 7.08 | 19.96 | 8.12 | 9.16 | 9E−03 |
| | 120 | 10.18 | 20.03 | 8.71 | 8.81 | 1E−02 |
| $S_{22}$ | 80 | 125.0 | 12.41 | 10.21 | 10.73 | 1E−01 |
| | 120 | 125.0 | 12.42 | 10.22 | 10.70 | 1E−01 |
| $S_{23}$ | 80 | 20.84 | 12.55 | 28.61 | 6.85 | 3E−04 |
| | 120 | 29.34 | 12.97 | 29.68 | 5.70 | 4E−04 |

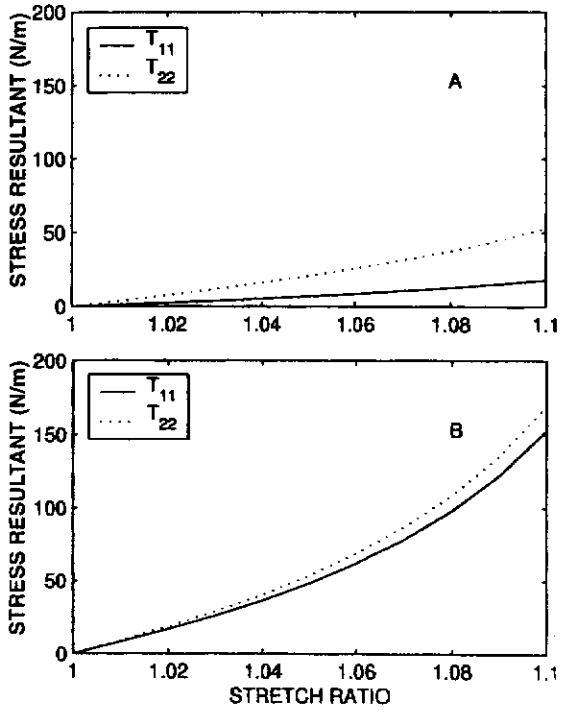


FIGURE 4 Predicted biaxial stress resultants *versus* stretch for specimen $S_1$. Results for region 1 are in panel A and those for region 2 are in panel B (note: $T_{11}$ is circumferential and $T_{22}$ meridional).

were near the fundus were the meridionally stiffer ones. Finally, Figures 6A and 6B show the predicted response for the same two sets of

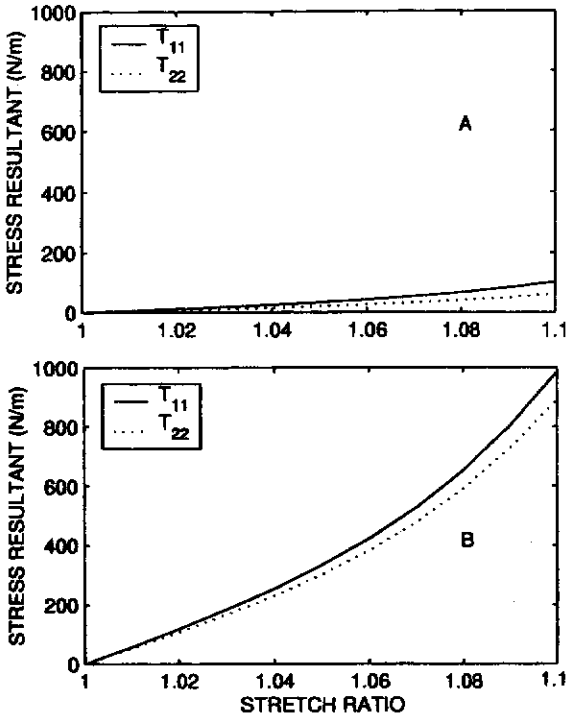


FIGURE 5 Similar to Figure 4 except for specimen $S_2$.

parameters, but for a uniaxial test (either $T_1 > 0$ and $T_2 = 0$ or $T_2 > 0$ and $T_1 = 0$). Again, the anisotropic response is evident.

## DISCUSSION

Despite many calls in the literature for information on the mechanical behavior of human saccular aneurysms, there are but three prior reports. Scott *et al.* [7] performed *in vitro* inflation (*i.e.*, pressure–volume) tests on seven human lesions and 16 nearby intracranial arteries. The aneurysms were assumed to be perfectly spherical, having deformed volumes of $4\pi a^3/3$ where $a$ is the deformed radius. This allowed the data to be presented as wall tension $T = Pa/2$ *versus* $\lambda^2 - 1$ (which is twice the Green strain, calculated based on assumed changes in surface area $= 4\pi(a^2 - A^2)/4\pi A^2$ where $A$ is the undeformed radius). Although this approach to data reduction provides but a gross measure of wall properties (*i.e.*, no information on possible anisotropy or heterogeneity),

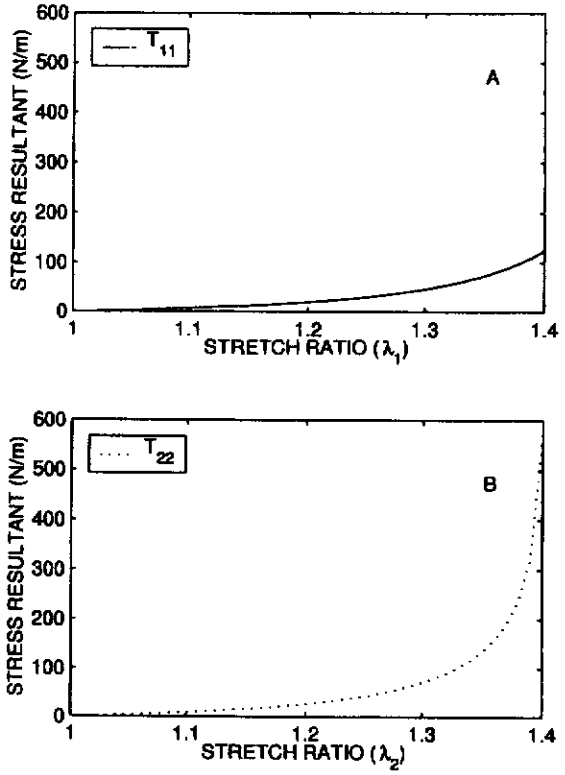


FIGURE 6 Predicted uniaxial results for one specimen up to a uniaxial stretch of 1.4.

Scott *et al.*, were the first to show that aneurysms exhibit a nonlinear response over finite strains. Steiger *et al.* [5] and Toth *et al.* [6] each reported stress–strain results from uniaxial tests on strips of tissue excised from the neck and fundus of human lesions. Uniaxial data are not sufficient, of course, for the quantification of multiaxial behavior. Nonetheless, both studies showed that the response differs between the two regions (specifically, the fundus failed at lower stretches than the neck) and that there is a marked anisotropy. Our findings support all of these general (qualitative) observations.

Perhaps the most striking difference between our results and those of Scott *et al.*, is the order of magnitude of the stress resultants (*i.e.*, tensions) under equibiaxial stretches. For example, Scott *et al.*, report stretches of 1.18 at a $P = 100$ mmHg and associated tensions on the order of 10 N/m. At stretches of 1.18, we compute tensions that are generally an order of magnitude larger. Indeed, this is expected given the experimental data in Figure 3, which reveals much smaller extensions at $P = 100$ mmHg. Although specimen-to-specimen differences could be the cause of the marked difference between the two studies, this seems unlikely given that results were consistent within each study from specimen-to-specimen. Rather, this is probably a result of differences in the unloaded reference configurations (note – assuming a membrane-type behavior disallows residual stresses, hence the traction-free configuration is the stress-free configuration). The volume-based method of Scott *et al.*, is likely less accurate than our marker-based determination, particularly given the advances in technology since 1972. Indeed personal communication with Dr. Roach suggested that their reference configuration could have been underestimated. This finding alone is particularly significant for it influences greatly the magnitudes of the stresses that are predicted by finite element (*e.g.* [9]) and other analyses (*e.g.* [17]). There will be a need to reconsider such analyses with the new sets of material parameters.

Unfortunately, neither Steiger *et al.*, nor Toth *et al.*, present actual uniaxial stress–strain curves to which we can compare our predictions (Figs. 5 and 6). Steiger *et al.*, did report failure stresses on the order of 0.5 to 1.2 MPa at uniaxial extensions of 1.37 and 1.57, respectively. Toth *et al.*, reported comparable values, a mean of 1.5 MPa at extensions of 1.45 or so. Our data did not address the rupture phenomenon for we desired to have an undamaged specimen available for subsequent histological analysis.

Although this is the first determination of the mechanical properties of human saccular aneurysms from multiaxial data, there are two primary shortcomings. First, due to the lack of axisymmetric lesions, we were not able to employ the method of Hsu *et al.* [8] to identify a form of the response functions directly from data. Hence, we had to resort to evaluating the ability of the Fung-type exponential relation to fit the data. Albeit a

good model, and widely used, this relation is limited in the degree of anisotropy it allows. As shown by Humphrey [13], the ratio of the principal stress resultants is necessarily constant for equibiaxial stretches, which is evident from Figures 4 and 5. Hence, although the relation appeared to fit the data reasonably well, there is a need to explore other candidate relations, which is best done via inflation tests on axisymmetric lesions. Second, we have results from only two lesions. Despite working with two medical centers, we have yet to procure additional unruptured juvenile lesions at autopsy within our set criterion of a maximum of 24 hours post-mortem.

In summary, based on these limited data, it appears that saccular aneurysms are much stiffer than suggested by the best data previously available (Scott *et al.*), and they do exhibit significant anisotropy and heterogeneity. Whether these variations in regional properties are the result of an attempt by the lesion to restore intramural stresses to near homeostatic levels is not clear [18], but this possibility merits closer scrutiny.

### *Acknowledgements*

This work was supported by a grant from the National Institutes of Health (HL 54957). We also wish to thank Professor P. B. Canham for thoughtful discussions and help in the procurement of specimens.

### *References*

[1] Ferguson, G. G. (1972). Physical factors in the initiation, growth and rupture of human intracranial saccular aneurysms. *J. Neurosurg.*, **37**, 666–677.

[2] Sekhar, L. N. and Heros, R. C. (1981). Origin, growth and rupture of saccular aneurysms: a review. *Neurosurg.*, **8**, 248–260.

[3] Stehbens, W. E. (1990). Pathology and pathogenesis of intracranial saccular berry aneurysms. *Neurol. Res.*, **12**, 29–34.

[4] Canham, P. B., Finlay, H. M. and Tong, S. Y. (1996). Stereological analysis of the layered collagen of human intracranial aneurysms. *J. Microscopy.*, **183**, 170–180.

[5] Steiger, H. J., Aaslid, R., Keller, S. and Reulen, H. J. (1989). Strength, elasticity and viscoelastic properties of cerebral aneurysms. *Heart and Vessels*, **5**, 41–46.

[6] Toth, M., Nadasy, G. L., Kerenyi, T., Orosz, M., Molnarka, G. and Monos, E. (1998). Sterically inhomogeneous viscoelastic behavior of human saccular cerebral aneurysms. *J. Vasc. Res.*, **35**, 345–355.

[7] Scott, S., Ferguson, G. G. and Roach, M. R. (1972). Comparison of the elastic properties of human intracranial arteries and aneurysms. *Can. J. Physiol. and Pharmacol.*, **50**, 328–332.

[8] Hsu, F. P. K., Schwab, C., Rigamonti, D. and Humphrey, J. D. (1994). Identification of response functions for nonlinear membranes via axisymmetric inflation tests: Implications for biomechanics. *Int. J. Sol. Struct.*, **31**, 3375–3386.

[9] Kyriacou, S. K. and Humphrey, J. D. (1996). Influence of size, shape and properties on the mechanics of axisymmetric saccular aneurysms. *J. Biomech.*, **29**, 1015–1022; *Erratum*, **30**, 761, 1997.

[10] Hsu, F. P. K., Downs, J., Liu, A. M. C., Rigamonti, D. and Humphrey, J. D. (1995). A triplane video-based experimental system for studying axisymmetrically inflated biomembranes. *IEEE Trans. Biomed. Engr.*, **42**, 442–449.

[11] McCulloch, A. D., Smaill, B. H. and Hunter, P. J. (1987). Left ventricular epicardial deformation in isolated arrested dog heart. *Am. J. Physiol.*, **252**, H233–241.

[12] Shah, A. D., Naff, N., Humphrey, J. D. and Rigamonti, D. (1999). Mechanical behavior of a vein-pouch saccular aneurysm model. *Neurol. Res.*, **21**, 569–573.

[13] Humphrey, J. D. (1999). An evaluation of pseudoelastic predictors used in arterial mechanics. *ASME J. Biomech. Engr.*, **121**, 259–262.

[14] Humphrey, J. D., Strumpf, R. K. and Yin, F. C. P. (1992). A constitutive theory for biomembranes: Application to epicardium. *ASME J. Biomech. Engr.*, **114**, 461–466.

[15] Seshaiyer, P. and Humphrey, J. D. (2000). A sub-domain inverse finite element characterization of hyperelastic membranes, including soft tissues (submitted).

[16] Humphrey, J. D. and Yin, F. C. P. (1986). Fiber-induced material behavior in composites. *Mech. Res. Comm.*, **13**, 277–283.

[17] Shah, A. D. and Humphrey, J. D. (1999). Finite strain elastodynamics of saccular aneurysms. *J. Biomech.*, **32**, 593–599.

[18] Ryan, J. M. and Humphrey, J. D. (1999). Finite element based predictions of preferred material symmetries in saccular aneurysms. *Ann. Biomed. Engr.*, **27**, 641–647.